Open- and closed-loop control of a turbulent round jet based on fluidic means

P. Zhang[2], H. L. Cao[3], J. Zhan[1] & Y. Zhou[2,3]

[1]Key Laboratory of Manufacture and Test Techniques for Automobile Parts, Ministry of Education, Chongqing University of Technology, Chongqing 400050, P. R. China

[2]Department of Mechanical Engineering, The Hong Kong Polytechnic University, Hung Hom, Kowloon, Hong Kong

[3]Shenzhen Postgraduate School, Harbin Institute of Technology, Shenzhen, China

INTRODUCTION

The concept to use control jets to enhance jet mixing was proposed by Davis [1], indicating that a jet may be controlled to achieve the optimized performance under different operation conditions. This work is a continuation of the study by Zhou et al. [2], who deployed two steady microjets to manipulate a round jet, and aims to control a turbulent jet using two unsteady microjets. The Reynolds number was made the same for the two investigations. So is the jet control facility. In the open-loop control, the dependence of jet decay on mass flow ratio C_m and excitation frequency ratio f_{ex}/f_0 of unsteady microjets to primary jet is investigated, where f_{ex} is the microjet excitation frequency and f_0 the preferred mode frequency in the uncontrolled jet. This is followed by the development of a closed-loop control.

RESULTS AND DISCUSSION

The jet facility consists of main-jet and microjet assemblies (see figure 1a & b), the latter including a stationary and a rotating disk both drilled with orifices. Once a stationary and a rotating orifice are aligned, an unsteady microjet emanates towards the main jet centreline. The Reynolds number was 8,000. The flow rate ratio C_m and excitation frequency ratio f_{ex}/f_0 of the microjets to the primary jet were varied from 0 to 15.4% and 0 to 1.41, respectively. A closed-loop controller was also developed, as shown in Figure 1c for experimental arrangement. Three wires were deployed in different positions of the injection plane. Feedback wire 1 was placed at $x/D = 2$ and $z/D = 0.3$, serving for detecting the vortex frequency $f_{x/D=2}$. Feedback wire 2 at $x/D = 3$ and $z/D = 0$ was used to capture the instantaneous centreline velocity $U_{x/D=3}$. Another wire was placed at $x/D = 5$ and $z/D = 0$ for monitoring the decay rate K. The controller acted on one hand to convert the $f_{x/D=2}$ value to the input voltage for the servo motor, which is linked to the frequency f_{ex} of unsteady microjets, and on the other hand to search $f_{x/D=2}$ corresponding to the minimum of $U_{x/D=3}$.

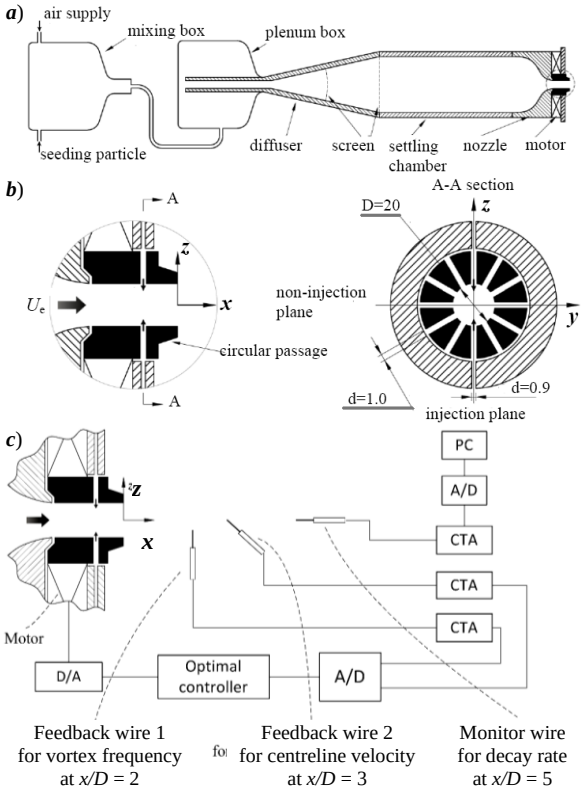

Figure 1. Schematic of jet control apparatus: (a) main jet assembly; (b) microjet assembly; (c) experimental arrangement for the closed-loop-controlled jet.

Following Zhou et al. [2], the jet decay rate K is estimated by $(U_e - U_{5D}) / U_e$, where U_{5D} is the centreline velocity at $x/D = 5$. Figure 2a presents the dependence of K on C_m which varies from 0 to 15.4% at a given frequency ratio of $f_{ex} / f_0 = 1.02$. Note that, the present jet response may be divided into three types, i.e., I (C_m < 2.0%), II (C_m = 2.0~4.0%), and III (C_m > 4.0). As shown in figure 2b, the decay rate at $C_m = 0.8\%$ is strongly dependent on f_{ex}/f_0, showing a twin-peak variation, one ($K = 0.144$) at $f_{ex}/f_0 = 0.66$ and the other ($K = 0.215$) at $f_{ex}/f_0 = 0.89$, along with a trough ($K = 0.130$) at $f_{ex}/f_0 = 0.77$ between the twin peaks.

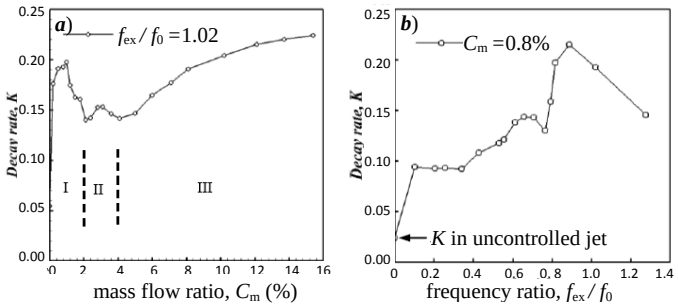

Figure 2. Dependence of jet decay rate on: (a) mass flow ratio C_m ($f_{ex} / f_0 = 1.02$); (b) excitation frequency ratio f_{ex} / f_0 ($C_m = 0.8\%$)

The flow in the controlled jet ($f_{ex} / f_0 = 1.02$) displays distinct flow characteristics in these types, as illustrated in figure 3. Except the case of $C_m = 10.2\%$ (see figure 3d & e), the rollup and presence of coherent structures are evident for x/D

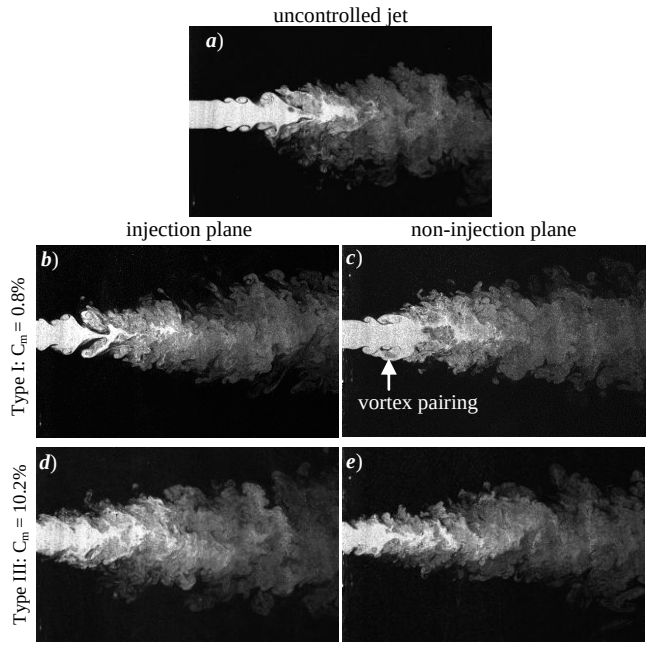

Figure 3. Photographs of typical flow structures captured from flow visualization in controlled jet (f_{ex}/f_0 = 1.02) for different C_m.

< 3.0. Vortex pairing is also discernible in the non-injection plane, as marked in figure 3c. Due to microjet forcing, vortices near the exit appear to be appreciably larger in scale in the injection plane (see figure3b) than in the uncontrolled jet (see figure 3a). Furthermore, vortices are relatively small in size in the non-injection plane (see figure 3c). The vortex pairing observed in the non-injection plane deserves attention. Two neigbouring vortex rings at x/D = 1.5 (C_m = 0.8%, see figure 3c) are undergoing a phase of mutual induction during a typical vortex pairing after the shear layer rolls up into vortices owing to Kelvin-Helmholtz instability. At C_m = 10.2% (type III), the flow appears turbulent in both planes even at x/D = 0 (see figure 3d & e). At large C_m, the two microjets in the injection plane penetrate deeply into the potential core, as observed by Davis [1], and even clash with each other around the centreline. The strong disturbance is partially transferred into the non-injection plane, eventually leading to the transition of laminar vortices to the turbulent in both planes. Being turbulent, the vortices entrain more ambient fluid into the jet and thereby recover a high vaule of K in type III, as suggested by Zhou et al. [2]. Thus, with increasing C_m, the jet gradually approaches a fully turbulent state with a bell-shaped rather than a top-hat mean velocity profile at jet exit and K approaches an asymptotic value.

Figure 4 presents the performances of the closed-loop controlled jet (C_m = 0.8%) when using different feedback signals. In the absence of the feedback signal from wire 2, $f_{x/D=2}/f_0$ (Fig 4a), albeit converged rapidly, drifted upward. However, once the feedback signal from wire 2 was introduced, which provides the information on instantaneous centreline velocity $U_{x/D=3}$ at x/D = 3, $f_{x/D=2}/f_0$ (Fig 4b) converged automatically and rapidly to the value almost the same as the optimal excitation frequency determined in the manual search of the open-loop control. The corresponding decay rate was 20.5%, very close to the maximum (21.5%) obtained in the open-loop control. The observation suggests the robustness of the technique.

CONCLUSIONS

1) The effects of the mass ratio on the control performance can be three types. Type I corresponds to very small mass ratio, and the perturbation excites the natural instability of jet, leading to significantly enhanced vortices, along with vortex pairing. The jet decay or entrainment rate is greatly modified and the control is highly effective. For Type III, the mass ratio is large and the two control jets penetrate deeply into the potential core and even clash with each other, resulting in the transition of laminar vortices to the turbulent in both planes. The jet decay rate increases and approaches an asymptotic state with increasing C_m, though the control may be less efficient than Type I. Type II is a transition between I and III, characterized by a medium mass ratio.

2) The jet decay rate depends strongly on the excitation frequency, showing one pronounced peak and one trough due to greatly enhanced and weakened vortices, respectively.

3) A closed-loop control is also developed and the optimal control performance can be achieved automatically, suggesting the robustness of the technique.

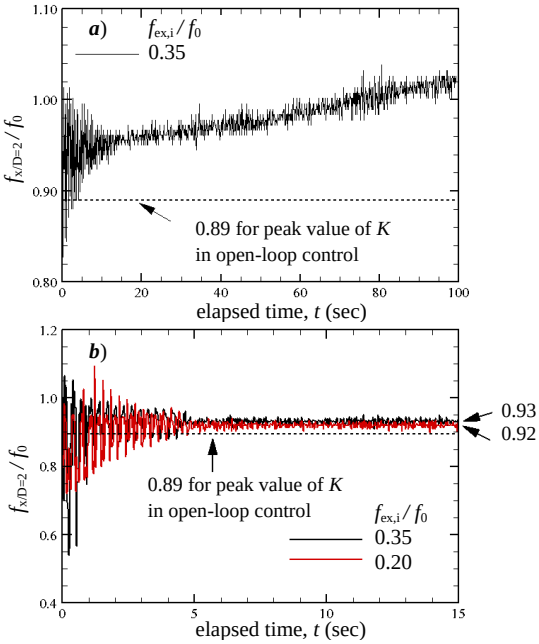

Figure 4. Performance of the closed-loop controlled jet (C_m = 0.8%): (a) time history of the frequency component $f_{x/D=2}/f_0$ of the signal from wire 1 in the absence of wire 2; (b) with both feedback signals deployed.

ACKNOWLEDGEMENT

YZ & JZ wish to acknowledge support given to him from Research Grants Council of HKSAR through grants PolyU 5350/10E and NSFC through grant 51275550.

REFERENCES

[1] Davis, M. R. (1982). Variable Control of Jet Decay. *AIAA J.* **20**, 606-609.

[2] Zhou, Y., Du, C., Mi, J. & Wang, X. W. (2012). Turbulent Round Jet Control Using Two Steady Minijets. *AIAA J.* **50**, 736-740.